

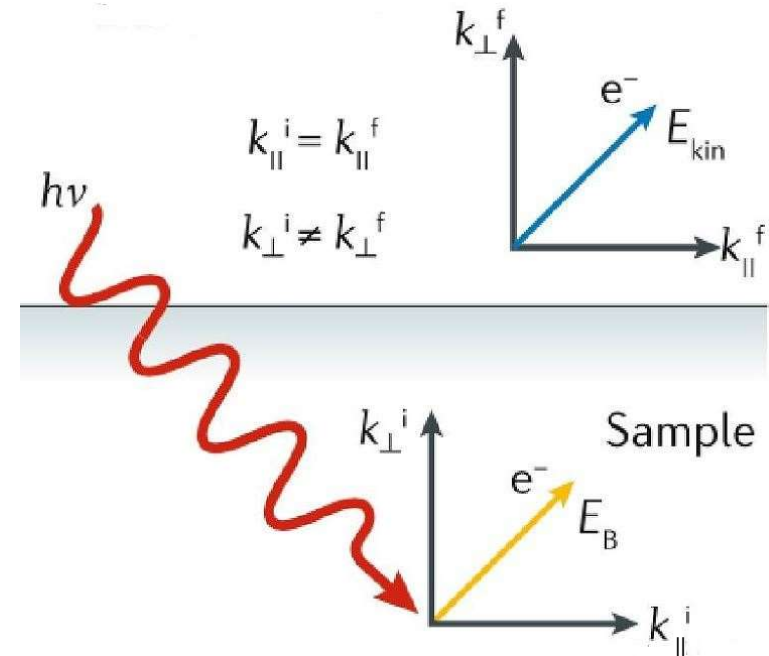
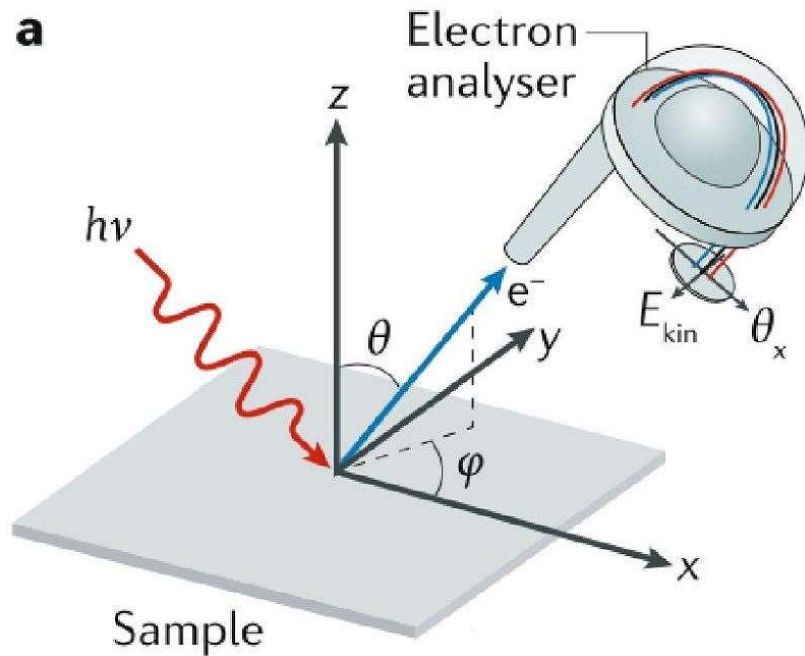
## Berry curvature near degenerate point

- 2D: [SS of TI](#), Graphene
- 3D: Weyl semimetal (later)

How to verify the Dirac cone of surface states?

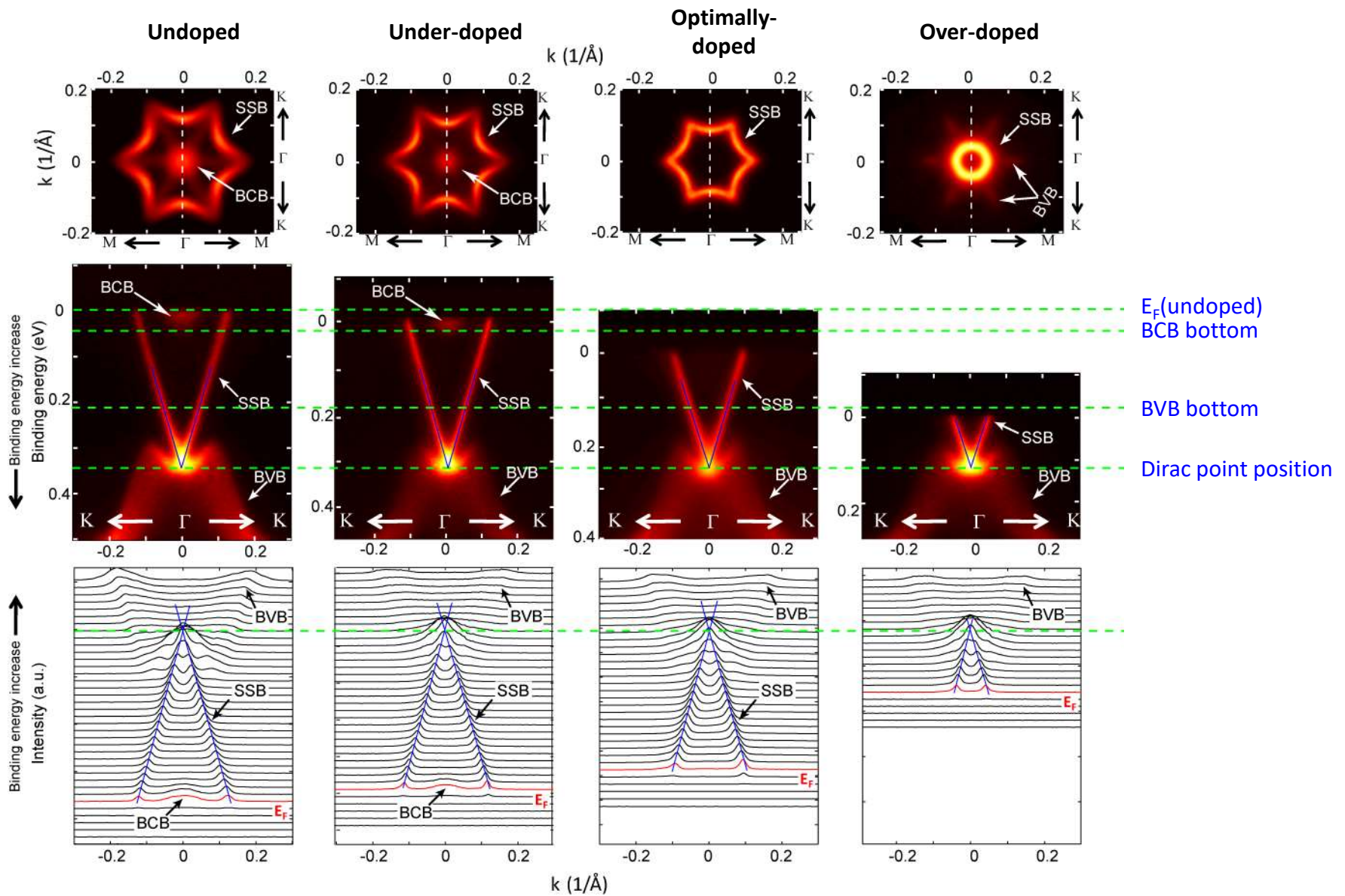
➔ Angle-Resolved Photo-Emission Spectroscopy (ARPES)

- Basically, it's photoelectric effect
- Can determine the energy dispersion of filled states
- Synchrotron radiation is used (20-100 eV)
- Sensitive to surface property (depth  $\sim 30$  Å), ideal for surface property and 2D material



# Arpes experiment on $\text{Be}_2\text{Te}_3$ surface states, Shen group

Doping evolution of the FS and band structure



# Effective Hamiltonian for the 2D surface state of 3D TI:

- Near the Dirac point.

Constraint from symmetry ( $T$ ,  $M$ , and  $C_3$ )

Fu PRL 2010

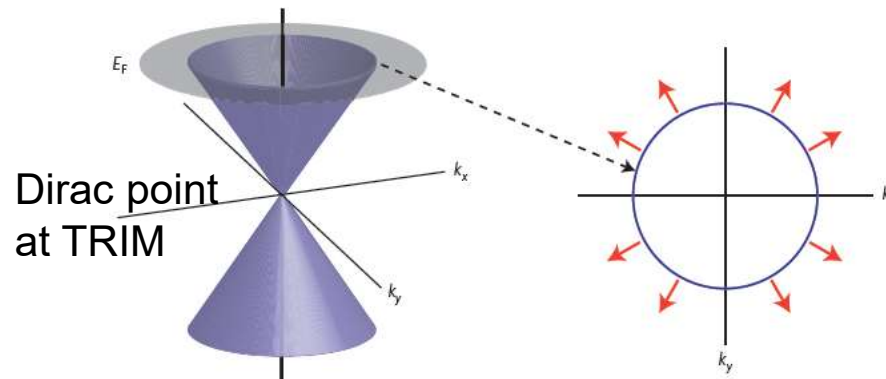
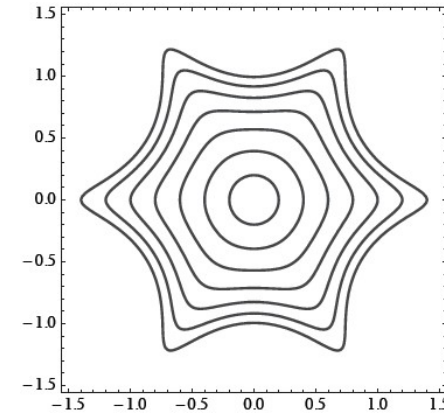
$$H(\vec{k}) = \varepsilon_0(\vec{k})I_{2 \times 2} + v_k(k_x \sigma_y - k_y \sigma_x) + \frac{\lambda}{2}(k_+^3 + k_-^3)\sigma_z$$

- To lowest order in  $k$ ,

$$H_{SS} = \alpha(\vec{k} \times \vec{\sigma})_z, \quad \langle \vec{\sigma} \rangle \perp \vec{k}$$

or  $H_{SS} = \alpha(\vec{k} \cdot \vec{\sigma})_z, \quad \langle \vec{\sigma} \rangle \parallel \vec{k}$

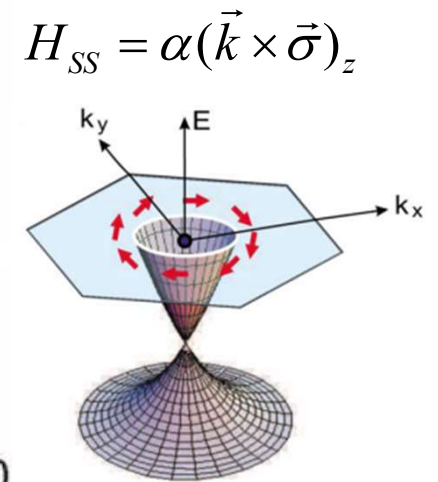
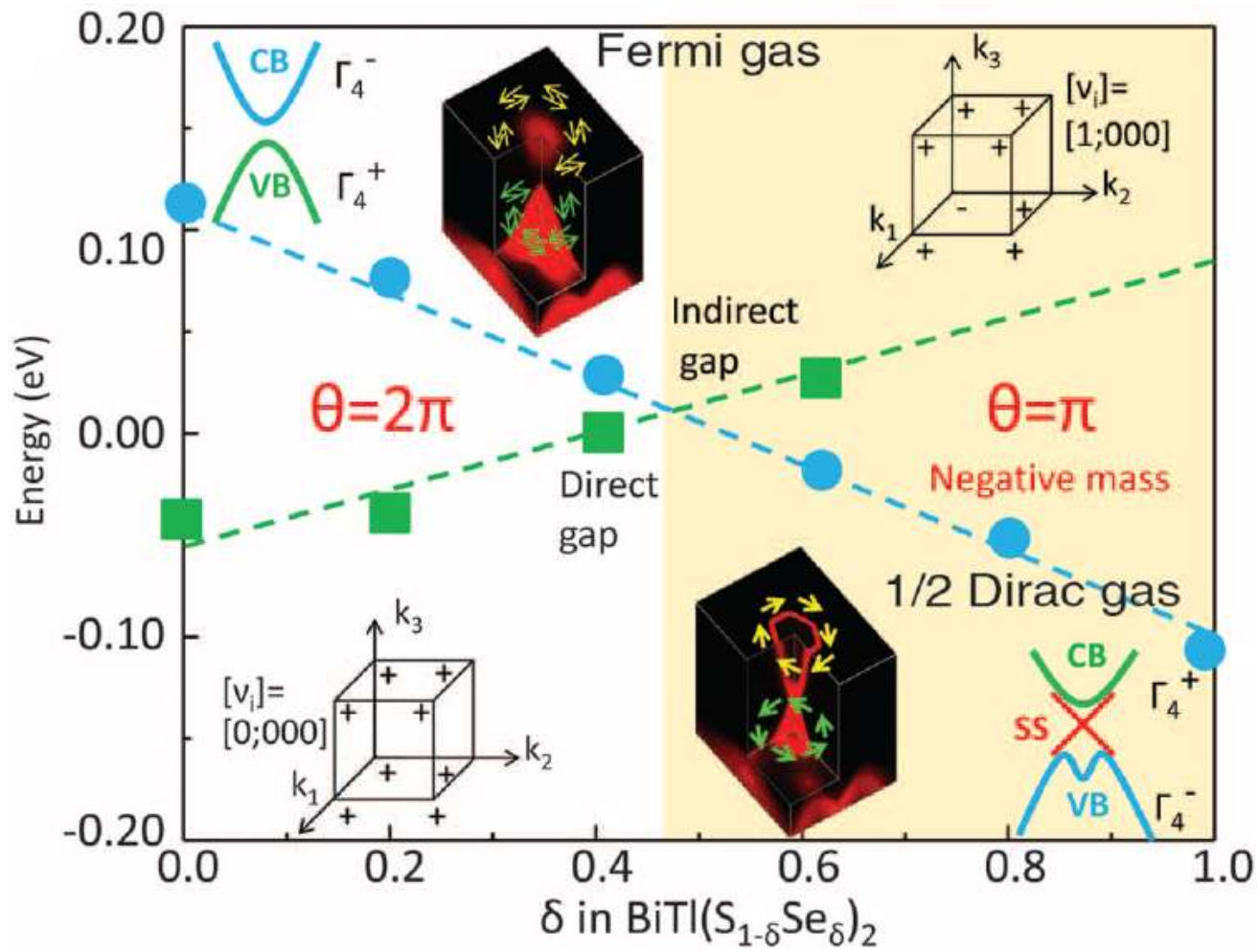
Warped Dirac cone



spin-momentum locking (Dirac cone with spin texture)

# Spin-resolved ARPES

Band inversion, parity change, emergence of SS, and spin-momentum locking



## Berry curvature in surface state Near a Dirac point

$$H_{SS} = \alpha(\boldsymbol{\sigma} \times \mathbf{k})_z + O(k^2)$$

$$\gamma_C = \mp \frac{\Omega_C}{2} = \mp \pi \quad \text{For a circle C around a DP}$$

➔  $F_z^\pm = \mp \pi \delta^2(\mathbf{k})$

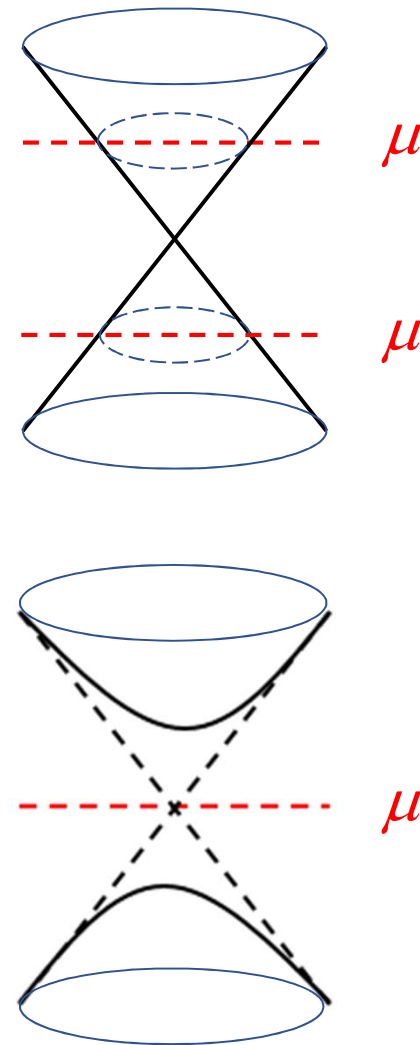
➔  $\sigma_H = 0$

- Open a gap by magnetization

HW 1  $H_{SS} = \alpha(\boldsymbol{\sigma} \times \mathbf{k})_z + m\sigma_z$

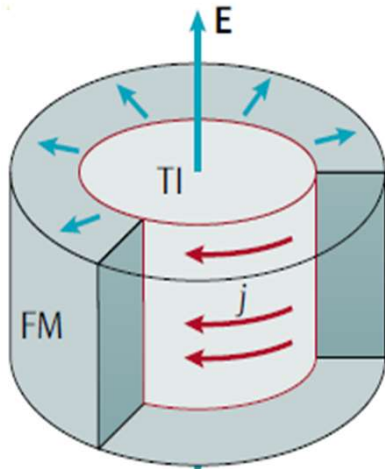
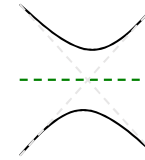
(a) ➔  $F_z^\pm = \mp \frac{\alpha^2 m}{2(m^2 + \alpha^2 k^2)^{3/2}}$

(b) ➔  $\sigma_H = \frac{e^2}{h} \frac{1}{2\pi} \int d^2k F_z^- = \frac{1}{2} \frac{e^2}{h}$



*Half-integer QHE*

# Electromagnetic response of TI surface state



Surface state  $\sim 2$  DEG

• Hall current  $J_H = \frac{e^2}{2h} E$

→ • Induced magnetization  $M = \frac{e^2}{2h} E$

Magnetoelectric (ME) coupling

→ Effective Lagrangian for EM wave

$$L_{EM} = L_0 + L_{axion}$$

$$L_0 = \frac{\epsilon_0}{2} (E^2 - c^2 B^2) - \rho\phi + \vec{J} \cdot \vec{A}$$

$$L_{axion} = \frac{e^2}{2h} \vec{E} \cdot \vec{B} = \sqrt{\frac{\epsilon_0}{\mu_0}} \alpha \frac{\Theta}{\pi} \vec{E} \cdot \vec{B}$$

fine structure constant

$$\alpha = \frac{1}{4\pi\epsilon_0} \frac{e^2}{\hbar c} \approx \frac{1}{137}$$

“axion” angle  $\Theta = \begin{cases} \pi & \text{for TI} \\ 0 & \text{for trivial} \end{cases}$   
 軸子



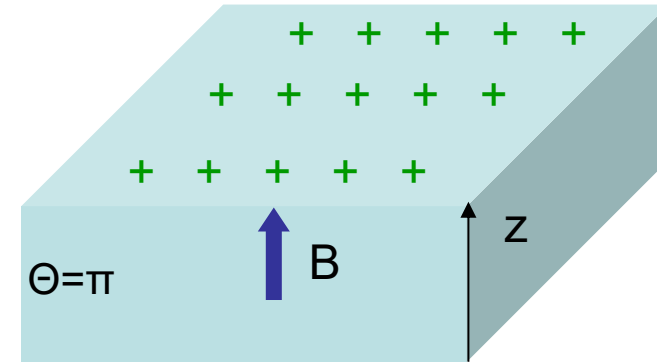
$\text{Cr}_2\text{O}_3$ :  $\theta \sim \pi/24$   
(TRS is broken)

A particle proposed by Wilczek *et al* to fix the strong CP problem

## Maxwell eqs with axion coupling (suppose $\epsilon, \mu$ are constants)

$$\left\{ \begin{array}{l} \nabla \cdot \left( \vec{E} + \alpha \frac{\Theta}{\pi} c \vec{B} \right) = \frac{\rho}{\epsilon} \\ \nabla \times \left( \vec{B} - \alpha \frac{\Theta}{\pi c} \vec{E} \right) = \mu \vec{J} + \frac{\partial}{c^2 \partial t} \left( \vec{E} + \alpha \frac{\Theta}{\pi} c \vec{B} \right) \\ \nabla \cdot \vec{B} = 0 \\ \nabla \times \vec{E} = -\frac{\partial}{\partial t} \vec{B} \end{array} \right.$$

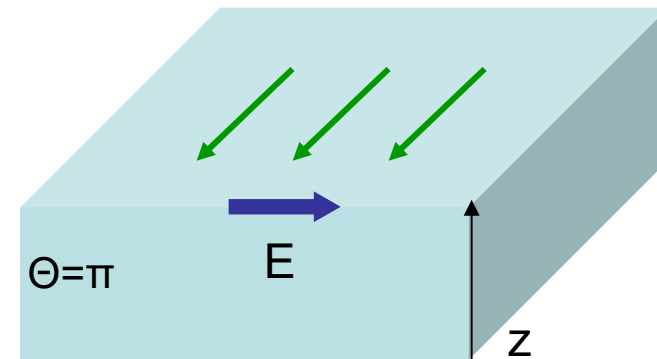
e.g.,  $\Theta(\vec{r}) = \pi h(-z)$



$$\rho_{\Theta} = c\alpha\epsilon\delta(z)B_z$$

## Effective charge and effective current

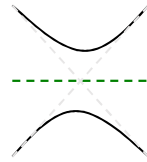
$$\left\{ \begin{array}{l} \nabla \cdot \vec{E} = \frac{\rho + \rho_{\Theta}}{\epsilon} \\ \rho_{\Theta} = -\frac{c\alpha\epsilon}{\pi} \nabla \cdot (\Theta \vec{B}) \\ \nabla \times \vec{B} = \mu (\vec{J} + \vec{J}_{\Theta}) + \frac{1}{c^2} \frac{\partial \vec{E}}{\partial t} \\ \vec{J}_{\Theta} = \frac{\alpha}{\pi c \mu} \nabla \times (\Theta \vec{E}) + \frac{\alpha}{\pi c \mu} \frac{\partial}{\partial t} (\Theta \vec{B}) \end{array} \right.$$



$$\vec{J}_{\Theta} = -\frac{\alpha}{c\mu} \delta(z) \hat{z} \times \vec{E} \rightarrow \sigma_{xy} = \frac{1}{2} \frac{e^2}{h}$$



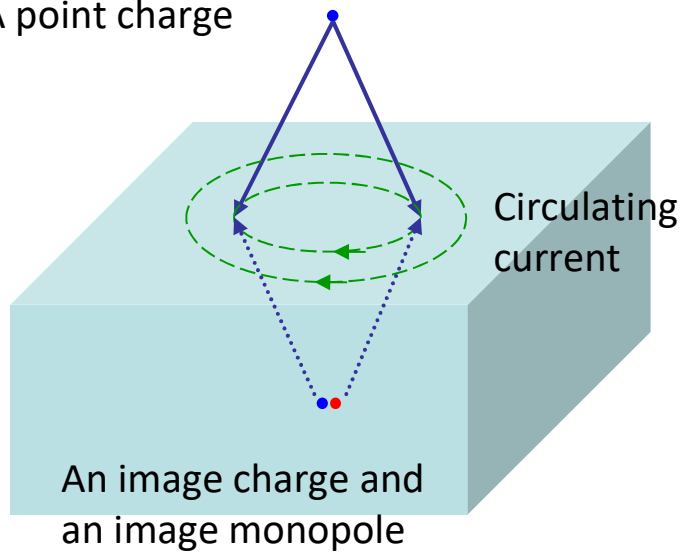
# Axion effect



## Static:

- Half-integer QHE
- Magnetic monopole in TI
- ...

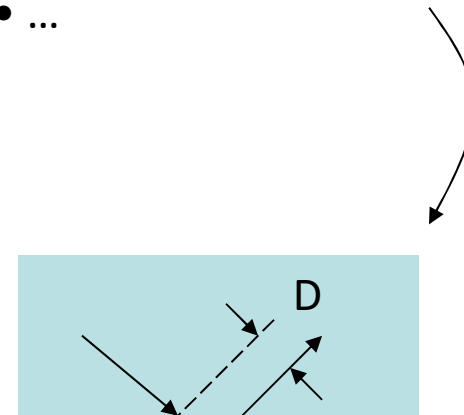
A point charge



Qi, Hughes, and Zhang, Science 2009

## Dynamic:

- Snell's law
- Fresnel formulas
- Brewster angle
- Goos-Hänchen effect
- ...



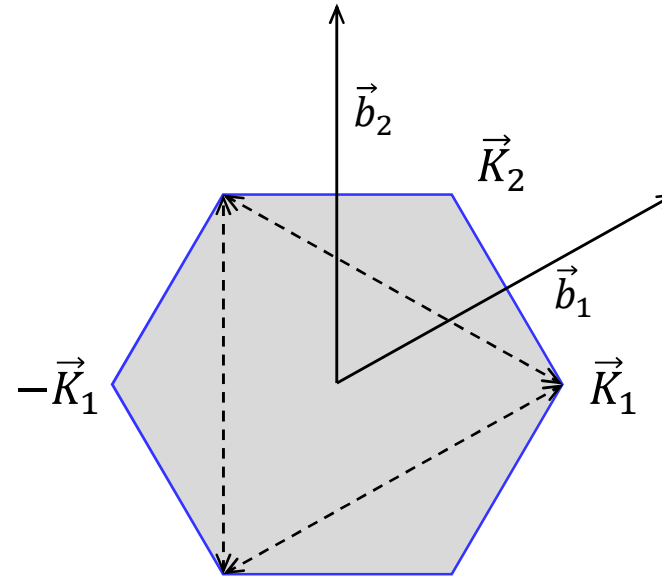
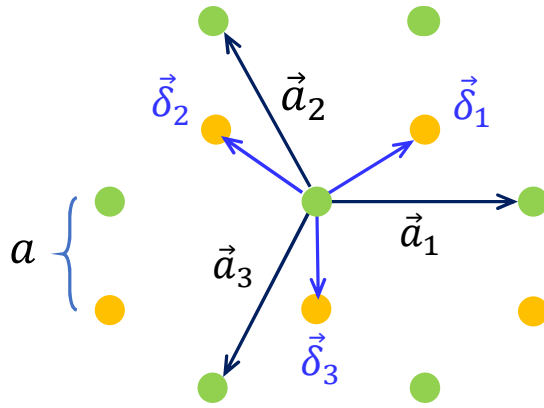
Longitudinal shift of reflected beam (total reflection)

Chang and Yang, PRB 2009

## Berry curvature near degenerate point

- 2D: SS of TI, [Graphene](#)
- 3D: Weyl semimetal (later)

## Graphene without spin



Brillouin zone

$$\hat{H} = \hat{H}_{NN} + \hat{H}_{NNN} + \hat{H}_{on-site}.$$

$$(1) \quad \hat{H}_{NN} = t_1 \sum_{\mathbf{R}} \left( d_{\mathbf{R}+\delta_1}^\dagger c_{\mathbf{R}} + d_{\mathbf{R}+\delta_2}^\dagger c_{\mathbf{R}} + d_{\mathbf{R}+\delta_3}^\dagger c_{\mathbf{R}} \right) + h.c.$$

$$(2) \quad \hat{H}_{NNN} = t_2 \sum_{\mathbf{R}} \left( c_{\mathbf{R}+\mathbf{a}_1}^\dagger c_{\mathbf{R}} + c_{\mathbf{R}+\mathbf{a}_2}^\dagger c_{\mathbf{R}} + c_{\mathbf{R}+\mathbf{a}_3}^\dagger c_{\mathbf{R}} \right) \\ + t_2 \sum_{\mathbf{R}} \left( d_{\mathbf{R}+\delta_1+\mathbf{a}_1}^\dagger d_{\mathbf{R}+\delta_1} + d_{\mathbf{R}+\delta_1+\mathbf{a}_2}^\dagger d_{\mathbf{R}+\delta_1} \right. \\ \left. + d_{\mathbf{R}+\delta_1+\mathbf{a}_3}^\dagger d_{\mathbf{R}+\delta_1} \right) + h.c.,$$

$$(3) \quad \hat{H}_{on-site} = \Delta \sum_{\mathbf{R}} c_{\mathbf{R}}^\dagger c_{\mathbf{R}} - \Delta \sum_{\mathbf{R}} d_{\mathbf{R}+\delta_1}^\dagger d_{\mathbf{R}+\delta_1}$$

Fourier  
transform

$$c_{\mathbf{R}} = \frac{1}{\sqrt{N}} \sum_{\mathbf{k}} e^{i\mathbf{k}\cdot\mathbf{R}} c_{\mathbf{k}}$$

$$d_{\mathbf{R}+\delta_1} = \frac{1}{\sqrt{N}} \sum_{\mathbf{k}} e^{i\mathbf{k}\cdot(\mathbf{R}+\delta_1)} d_{\mathbf{k}}$$

Orthogonal relation

$$\sum_{\mathbf{R}} e^{i(\mathbf{k}'-\mathbf{k})\cdot\mathbf{R}} = N\delta_{\mathbf{k}'\mathbf{k}}.$$

e.g.,

$$\sum_{\mathbf{R}} d_{\mathbf{R}+\delta_1}^\dagger c_{\mathbf{R}} = \frac{1}{N} \sum_{\mathbf{k},\mathbf{k}'} \sum_{\mathbf{R}} e^{-i(\mathbf{k}'-\mathbf{k})\cdot\mathbf{R}} e^{-i\mathbf{k}'\cdot\delta_1} d_{\mathbf{k}'}^\dagger c_{\mathbf{k}}$$

$$= \sum_{\mathbf{k}} e^{-i\mathbf{k}\cdot\delta_1} d_{\mathbf{k}}^\dagger c_{\mathbf{k}},$$



$$\hat{H} = t_1 \sum_{\mathbf{k}} (e^{-i\mathbf{k}\cdot\delta_1} + e^{-i\mathbf{k}\cdot\delta_2} + e^{-i\mathbf{k}\cdot\delta_3}) d_{\mathbf{k}}^\dagger c_{\mathbf{k}}$$

$$+ t_2 \sum_{\mathbf{k}} (e^{-i\mathbf{k}\cdot\mathbf{a}_1} + e^{-i\mathbf{k}\cdot\mathbf{a}_2} + e^{-i\mathbf{k}\cdot\mathbf{a}_3}) c_{\mathbf{k}}^\dagger c_{\mathbf{k}}$$

$$+ t_2 \sum_{\mathbf{k}} (e^{-i\mathbf{k}\cdot\mathbf{a}_1} + e^{-i\mathbf{k}\cdot\mathbf{a}_2} + e^{-i\mathbf{k}\cdot\mathbf{a}_3}) d_{\mathbf{k}}^\dagger d_{\mathbf{k}} + h.c.$$

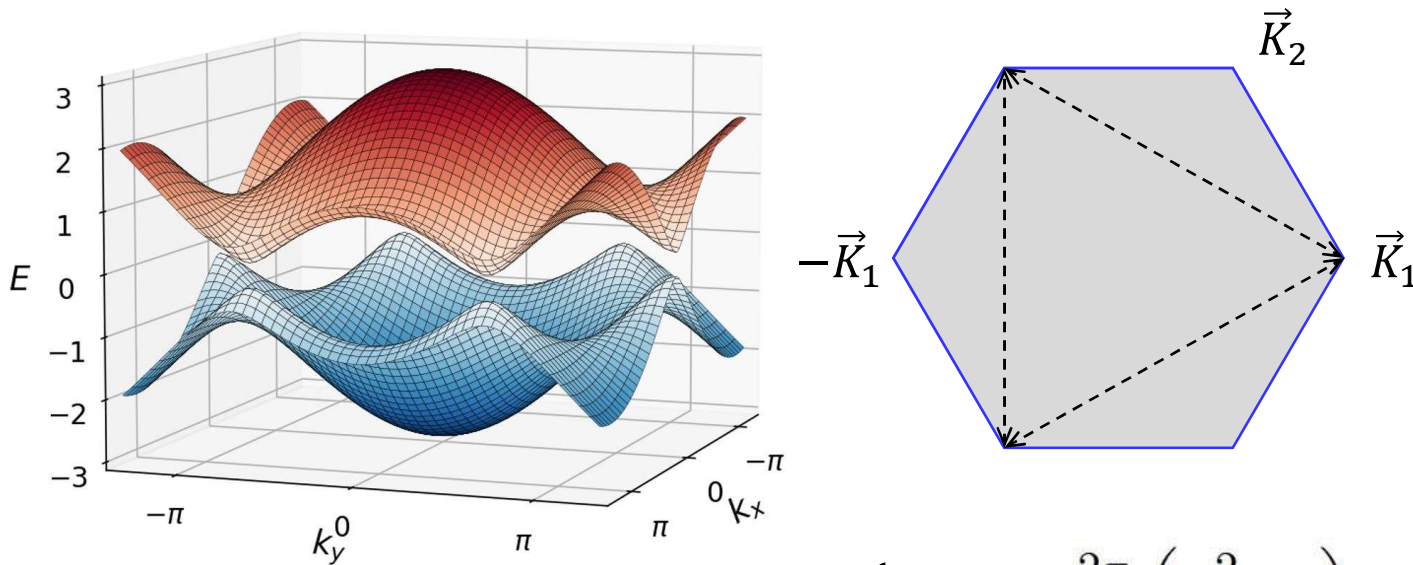
$$+ \Delta \sum_{\mathbf{k}} (c_{\mathbf{k}}^\dagger c_{\mathbf{k}} - d_{\mathbf{k}}^\dagger d_{\mathbf{k}})$$

$$= \sum_{\mathbf{k}} \begin{pmatrix} c_{\mathbf{k}}^\dagger & d_{\mathbf{k}}^\dagger \end{pmatrix} H(\mathbf{k}) \begin{pmatrix} c_{\mathbf{k}} \\ d_{\mathbf{k}} \end{pmatrix}.$$

$$\begin{aligned}
 H(\mathbf{k}) &= \begin{pmatrix} 2t_2 \sum_i \cos \mathbf{k} \cdot \mathbf{a}_i + \Delta & t_1 \sum_i e^{i\mathbf{k} \cdot \delta_i} \\ t_1 \sum_i e^{-i\mathbf{k} \cdot \delta_i} & 2t_2 \sum_i \cos \mathbf{k} \cdot \mathbf{a}_i - \Delta \end{pmatrix} \\
 &= h_0(\mathbf{k}) + \mathbf{h}(\mathbf{k}) \cdot \boldsymbol{\sigma},
 \end{aligned}$$

➔  $\varepsilon_{\pm}(\mathbf{k}) = h_0(\mathbf{k}) \pm |\mathbf{h}(\mathbf{k})|$

$$|\mathbf{h}| = \sqrt{3t_1^2 + 2t_1^2 (\cos \mathbf{k} \cdot \mathbf{a}_1 + \cos \mathbf{k} \cdot \mathbf{a}_2 + \cos \mathbf{k} \cdot \mathbf{a}_3) + \Delta^2}$$



Gapless (Dirac point) at

$$\begin{cases} \mathbf{K}_1 = \frac{2\pi}{a} \left( \frac{2}{3\sqrt{3}}, 0 \right), \\ \mathbf{K}_2 = \frac{2\pi}{a} \left( \frac{1}{3\sqrt{3}}, \frac{1}{3} \right) \end{cases} \text{ or } -\mathbf{K}_1$$

## Effective Hamiltonian near Dirac point

$$\mathbf{k} = \mathbf{K}_i + \mathbf{k}_i, \quad |\mathbf{k}_i| \ll |\mathbf{K}_i|; \quad i = 1, 2.$$

$$H_{12}(\mathbf{k}) = t_1 \left( e^{i\mathbf{K}_1 \cdot \boldsymbol{\delta}_1} e^{i\mathbf{k}_1 \cdot \boldsymbol{\delta}_1} + e^{i\mathbf{K}_1 \cdot \boldsymbol{\delta}_2} e^{i\mathbf{k}_1 \cdot \boldsymbol{\delta}_2} + e^{i\mathbf{K}_1 \cdot \boldsymbol{\delta}_3} e^{i\mathbf{k}_1 \cdot \boldsymbol{\delta}_3} \right)$$

	$i = 1$	2	3
$\mathbf{K}_1 \cdot \boldsymbol{\delta}_i =$	$+\frac{2\pi}{3}$	$-\frac{2\pi}{3}$	0
$\mathbf{K}_2 \cdot \boldsymbol{\delta}_i =$	$-\frac{2\pi}{3}$	$+\frac{2\pi}{3}$	0
$e^{i\mathbf{K}_{1/2} \cdot \boldsymbol{\delta}_i} =$	$-\frac{1}{2} \mp \frac{\sqrt{3}}{2}i$	$-\frac{1}{2} \pm \frac{\sqrt{3}}{2}i$	1

$$\begin{aligned} \rightarrow H(\mathbf{k}) &\simeq \begin{pmatrix} \Delta & \frac{3}{2}t_1a(\pm k_x - ik_y) \\ \frac{3}{2}t_1a(\pm k_x + ik_y) & -\Delta \end{pmatrix} \\ &= \boxed{\hbar v_F(\tau k_x \sigma_x + k_y \sigma_y) + \Delta \sigma_z}, \end{aligned}$$

$\tau \equiv \pm$  for  $\pm K_1$     2 inequivalent Dirac “valleys”

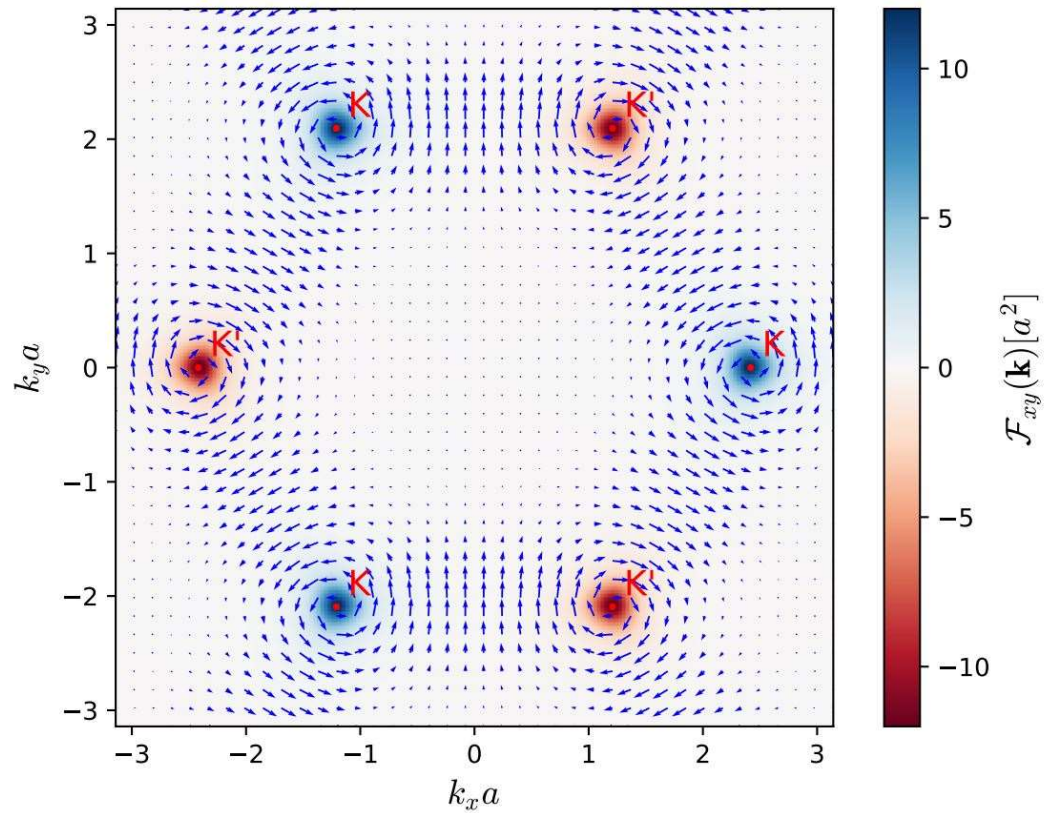
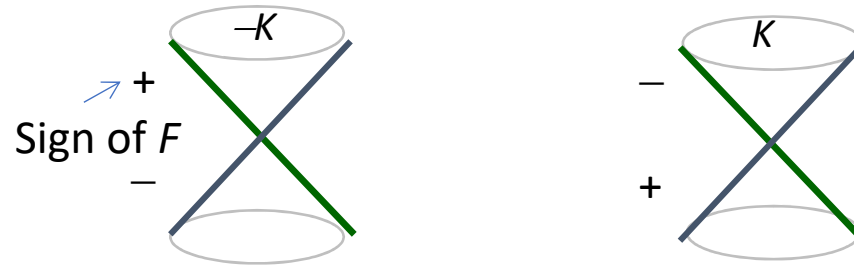
Berry curvature  $F_z^\pm(\mathbf{k}) = \mp \frac{1}{2\hbar^3} \mathbf{h} \cdot \frac{\partial \mathbf{h}}{\partial k_x} \times \frac{\partial \mathbf{h}}{\partial k_y}.$

# Berry curvature

Near Dirac point

$$F_{z\tau}^{\pm}(\mathbf{K}_1) = \pm\tau \frac{9}{8} \frac{a^2 t_1^2 \Delta}{h^3} = \pm\tau \frac{1}{2} \frac{\hbar^2 v_F^2 \Delta}{h^3}$$

Conduction band and valence band have opposite Berry curvatures

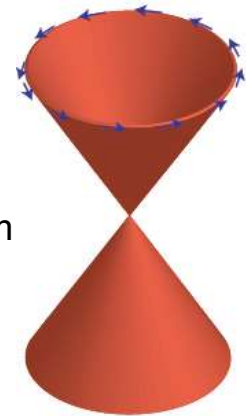
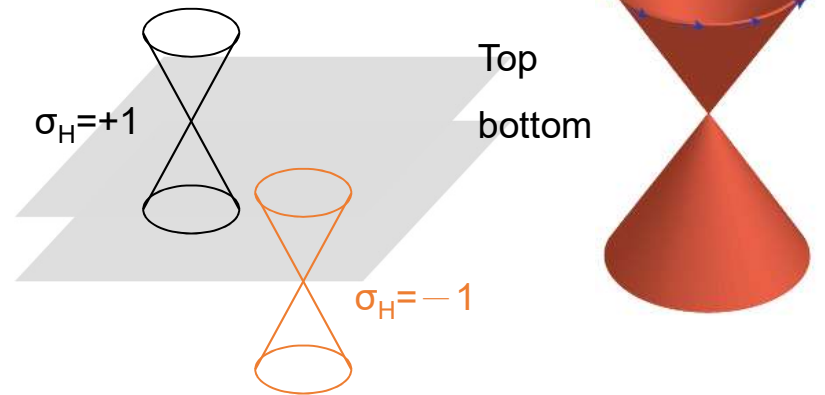
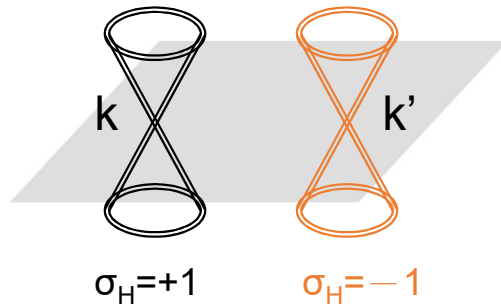
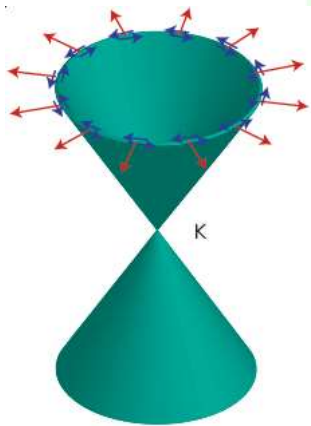


Dirac point:  
Graphene

vs.

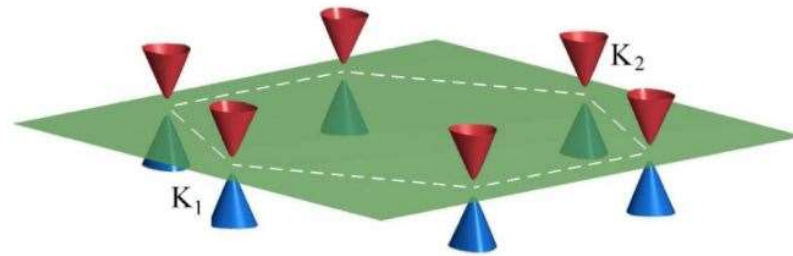
Topological insulator

even number	odd number (on one side)
located at Fermi energy	not located at $E_F$
half integer QHE ( $\times 4$ )	half integer QHE (if $E_F$ is located at DP)
spin is not locked with $k$	spin is locked with $k$
can be opened by substrate (DP protected by TRS + SIS)	<i>cannot</i> be opened if there is TRS

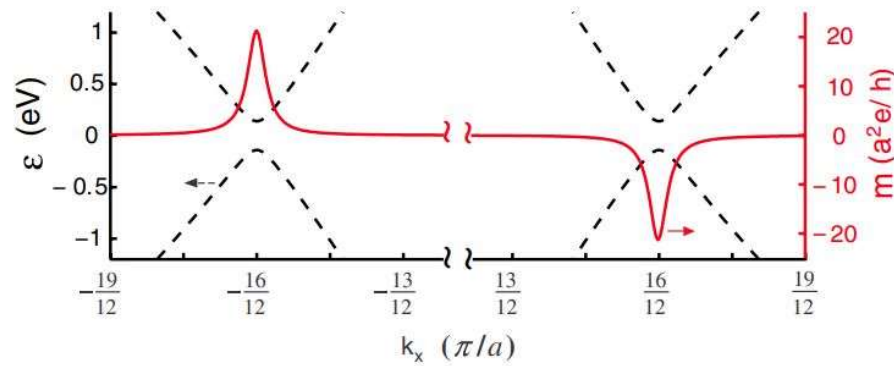




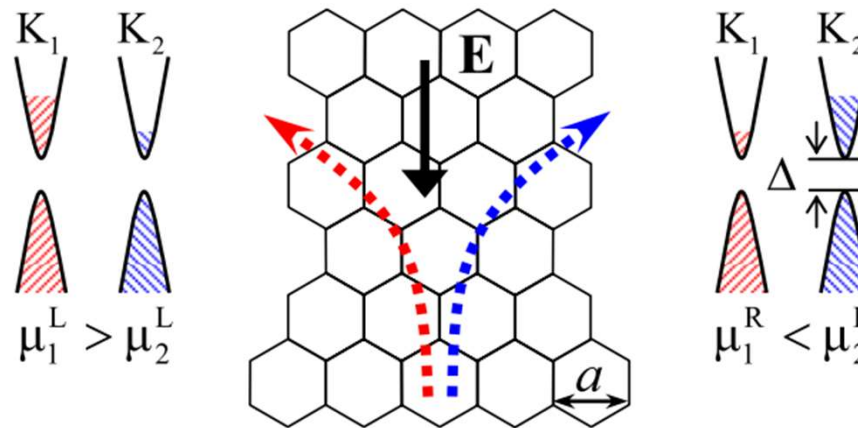
# Valley Hall effect (Xiao et al, PRL 2007)



**$B=0$  !**



$\Omega \sim m$   
Orbital magnetic moment



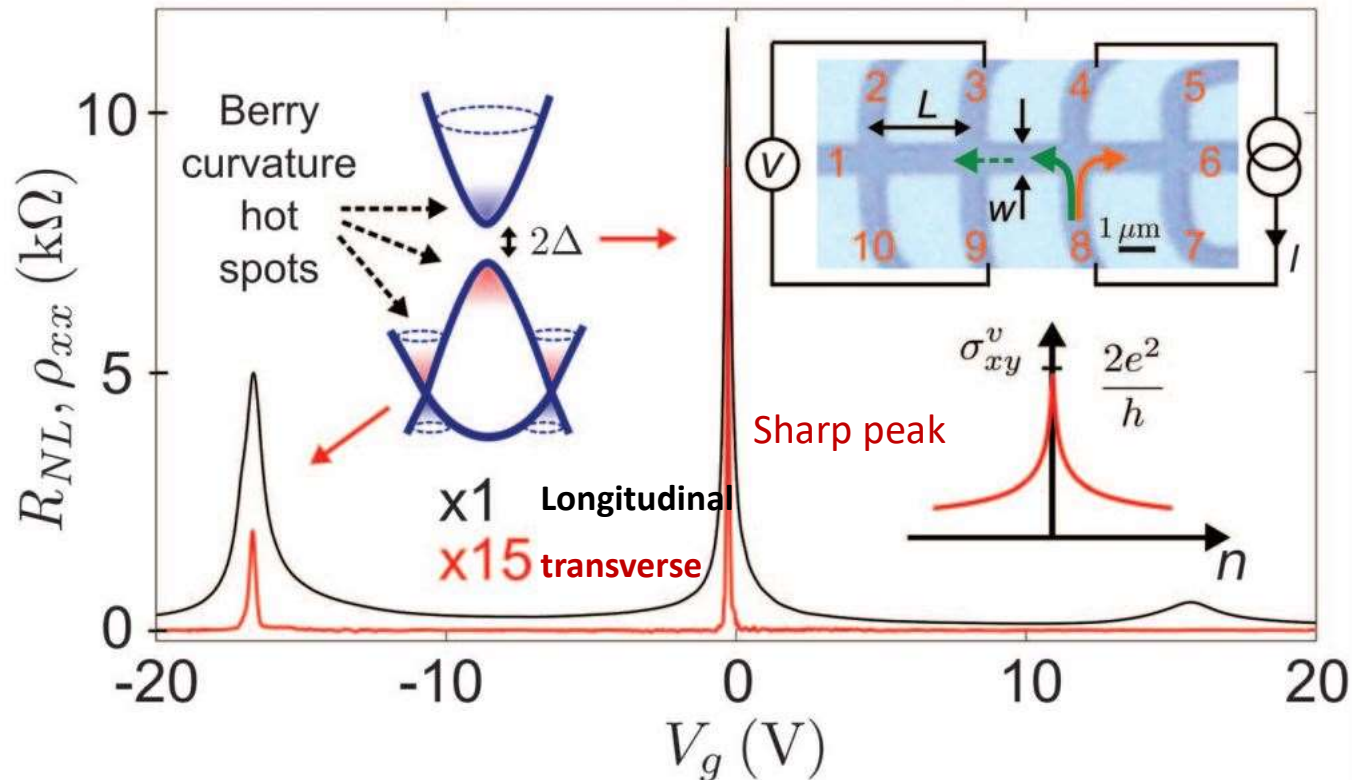
Opposite Lorentz-like forces

# Detecting topological currents in graphene superlattices

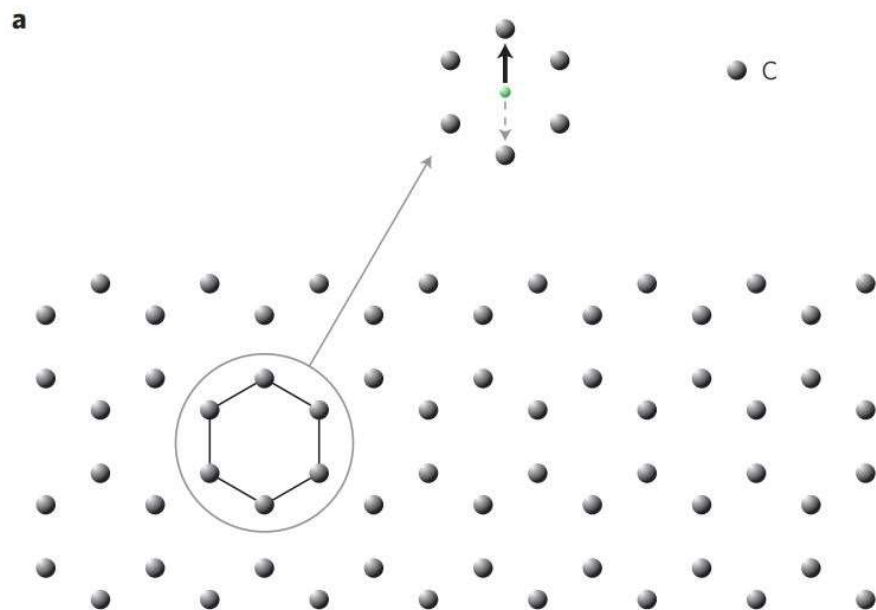
Science, 2014

R. V. Gorbachev,<sup>1,2\*</sup> J. C. W. Song,<sup>3,4\*</sup> G. L. Yu,<sup>1</sup> A. V. Kretinin,<sup>2</sup> F. Withers,<sup>2</sup> Y. Cao,<sup>1</sup> A. Mishchenko,<sup>1</sup> I. V. Grigorieva,<sup>2</sup> K. S. Novoselov,<sup>2</sup> L. S. Levitov,<sup>3\*</sup> A. K. Geim<sup>1,2†</sup>

Graphene on hBN (breaking inversion sym,  $E_g=30$  meV)

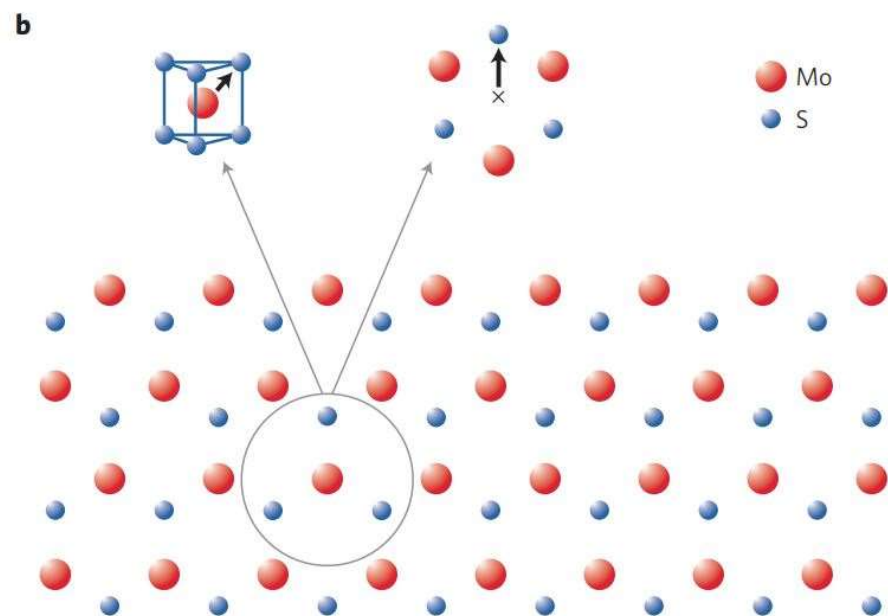


### Graphene (with SIS)



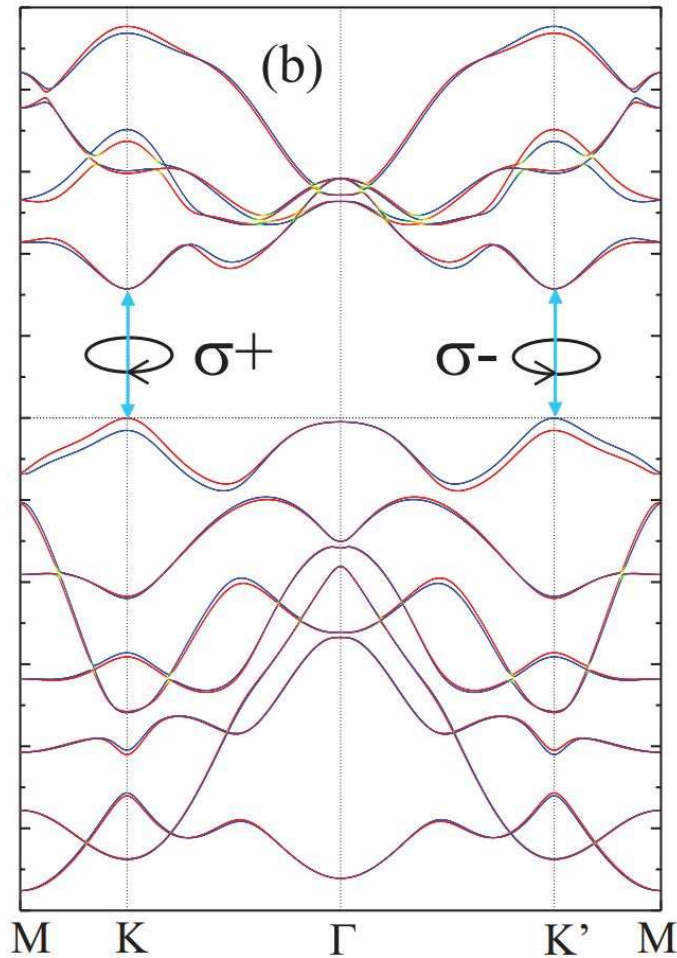
Graphene on hBN breaks SIS,  
opens a gap  $\sim 30$  mV

### monolayer MoS<sub>2</sub> (without SIS)



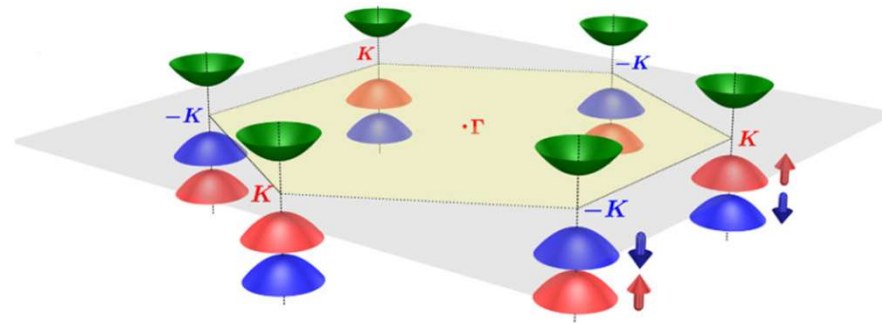
An energy gap  $\sim 1.9$  eV  
(easier for optical and electrical control)

## Band structure for MoS<sub>2</sub>



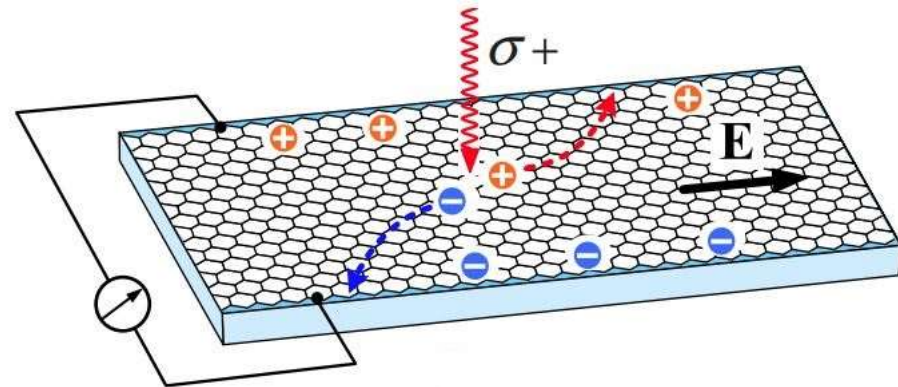
Opposite valleys have opposite BC and opposite magnetic moment

Feng et al, PRB 2012



- $K, K'$  population imbalance induced by optical pumping
- net Hall current

photo-induced AHE



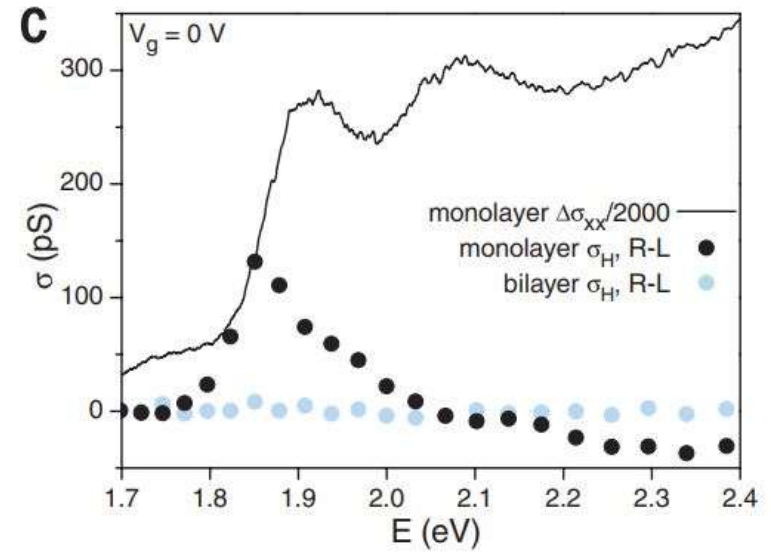
Electron and hole (in the same valley) contribute to the same current

VALLEYTRONICS

Science, 2014

# The valley Hall effect in MoS<sub>2</sub> transistors

K. F. Mak,<sup>1,2\*</sup> K. L. McGill,<sup>2</sup> J. Park,<sup>1,3</sup> P. L. McEuen<sup>1,2\*</sup>



Local Kerr signal

Lee et al, Nature  
Nano Tech, 2016

